Fully Current-Based Sub-Bandgap Optoelectronic Differential Ideality Factor Technique and Extraction of Subgap DOS in Amorphous Semiconductor TFTs

Hagyoul Bae, Hyojoon Seo, Sungwoo Jun, Hyunjun Choi, Jaeyeop Ahn, Junseok Hwang, Jungmin Lee, Saeroonter Oh, Jong-Uk Bae, Sung-Jin Choi, Dae Hwan Kim, *Senior Member, IEEE*, and Dong Myong Kim

***Abstract*— A sub-bandgap optoelectronic differential ideality factor technique is proposed for extraction of the intrinsic density-of-states (DOS) over the bandgap in amorphous semiconductor thin-film transistors (TFTs). In the proposed technique, the gate bias-dependent differential change in the difference of ideality factors ($d\Delta\eta(V_{GS})/dV_{GS}$) between dark and sub-bandgap photonic excitation condition is employed. With the sub-bandgap photons ($h\nu < E_g$), the photonic excitation of electrons is confined only from the localized DOS over the bandgap. We applied the proposed technique to a-InGaZnO TFTs with $W/L = 50/25$ μm/μm and extracted the energy distribution of the intrinsic DOS for the localized states over the bandgap.**

***Index Terms*— Amorphous oxide semiconductor, density-of-states (DOS), differential ideality factor, InGaZnO (IGZO), optoelectronic, subgap thin-film transistor (TFT), subthreshold, TFT.**

I. Introduction

AMORPHOUS oxide semiconductor (AOS) thin-film transistors (TFTs) are under the active research and development for display systems due to the high carrier mobility, the large-area uniformity, the deposition process at a low temperature, and the visible light transparency. Extraction of the subgap density-of-states [DOS; $g(E)$] over the bandgap ($E_V < E < E_C$) in amorphous semiconductors is very important and crucial in robust characterization and modeling of AOS TFTs [1]–[3]. There are various techniques for characterization of DOS such as the capacitance–voltage (C–V), current–voltage (I–V), and other characterization techniques [4]–[7]. They require a complicated calculation or cause a drift of inherent properties by the thermal and/or electrical stress during characterization [8]. We also note that C–V-based characterization has its own limit of the application to large area devices while I–V-based technique can be applied to characterize even extremely small devices due to high current sensitivity of the characterization system. In the previous work, we obtained the intrinsic $g(E)$ by using the frequency dispersive C–V characteristics of TFTs [7]. As the device size decreases, C–V-based extraction techniques cause errors due to parasitic resistances and capacitances in the characterization.

In this brief, we propose a sub-bandgap optoelectronic differential ideality factor technique (SODIFT) for extraction of $g(E)$ by the optoelectronic response of the differential change of the ideality factors $d\Delta\eta(V_{GS})/dV_{GS}$ under sub-bandgap ($E_{ph} = h\nu < E_g$) photonic excitation with the energy less than the bandgap of the active region. Under sub-bandgap optical excitation, electrons are excited only from the photo-responsive subgap states ($E_C - E_{ph} < E < E_F$) to the conduction band. By the differential change in the difference of ideality factors under dark and photonic excitation, the intrinsic DOS for the localized states is fully separated from the contribution by free electrons especially for the gate bias close to the threshold voltage (V_T). This allows efficient extraction of the intrinsic DOS only from the DOS excluding the contribution from free electrons. We also expect that the proposed I–V-based SODIFT extraction technique is useful for modeling and characterization of AOS TFTs with extremely small feature size.

II. Sub-Bandgap Optoelectronic Differential Ideality Factor Technique for Intrinsic DOS

Fig. 1(a) shows a setup for C–V-based characterization of the subgap DOS under photonic state. The schematic

Manuscript received May 16, 2014; revised July 16, 2014; accepted August 11, 2014. Date of publication September 4, 2014; date of current version September 18, 2014. This work was supported in part by the National Research Foundation of Korea through the Ministry of Education, Science and Technology, Korean Government, under Grant 2013R1A2A2A05005472 and Grant 2012-0000147, in part by the BK21+ Program, in part by the Global Ph.D. Fellowship Program through the Ministry of Education, National Research Foundation of Korea, under Grant 2014H1A2A1022137, in part by the SILVACO, and in part by the IC Design Education Center for the CAD software. The review of this brief was arranged by Editor J. Huang.

H. Bae was with Kookmin University, Seoul 136-702, Korea. He is now with the Department of Electrical Engineering, Korea Advanced Institute of Science and Technology, Daejeon 305-701, Korea.

H. Seo, S. Jun, H. Choi, J. Ahn, J. Hwang, J. Lee, S.-J. Choi, D. H. Kim, and D. M. Kim are with the School of Electrical Engineering, Kookmin University, Seoul 136-702, Korea (e-mail: dmkim@kookmin.ac.kr).

S. Oh and J.-U. Bae are with the LG Display Research and Development Center, Paju 413-811, Korea.

Color versions of one or more of the figures in this paper are available online at http://ieeexplore.ieee.org.

Digital Object Identifier 10.1109/TED.2014.2348592

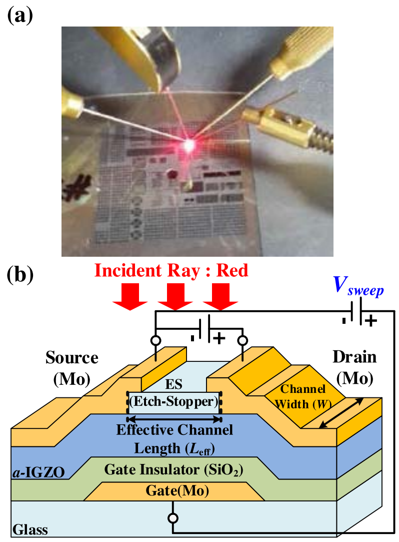

Fig. 1. (a) Measurement setup for photonic I–V characterization. (b) Device structure and cross sectional view of a-IGZO TFTs.

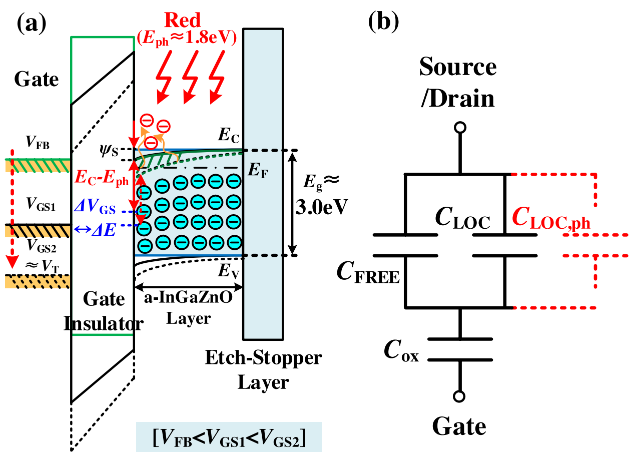

Fig. 2. (a) Energy band diagram under sub-bandgap optical illumination. The photo-responsive energy range ($E_C - E_{\rm ph} < E < E_F$) can be modulated by $V_{\rm GS}$. (b) Capacitance model including $C_{\rm LOC,ph}$ as the capacitance from the photo-excited carriers.

view of a-InGaZnO (IGZO) TFTs with inverted staggered bottom-gate structure is shown in Fig. 1(b). An energy band diagram of a-IGZO TFTs is shown in Fig. 2(a) with capacitive equivalent circuit in Fig. 2(b). The sub-bandgap optical source is guided over the a-IGZO active region of the device through a multimode fiber with diameter $d = 50\ \mu$m. An optical source with a sub-bandgap photon energy ($\lambda_R = 656$ nm, $E_{{\rm ph},R} = 1.89$ eV $< E_{g,{\rm IGZO}} \approx 3$ eV, and optical power $P_{{\rm opt},R} = 10$ mW) is employed to pump the trapped electrons in the active channel region from the photo-responsive subgap states ($(E_C - E_{\rm ph}) < E < E_F$) to the conduction band ($E > E_C$). We note that the charges from bulk traps derived from a specific $V_{\rm GS}$ corresponds to that from a specific surface potential (ψ_S) or energy level over the bandgap ($E_{g,{\rm IGZO}} \approx 3$ eV). Therefore, the optically excited charges ($Q_{\rm LOC}(V_{\rm GS})$) for the differential gate voltage ($\Delta V_{\rm GS}$ or ψ_S) result from the specific trap energy level (E_t) over $(E_F - E_{\rm ph})(V_{{\rm GS},i}) < E_t < (E_F - E_{\rm ph})(V_{{\rm GS},i+1})[i = 1, 2, 3 \ldots]$. The gate capacitance ($C_G$) is in a series of the $V_{\rm GS}$-independent oxide capacitance ($C_{\rm ox}$) with the $V_{\rm GS}$-dependent substrate capacitance ($C_S(V_{\rm GS})$). As also shown in Fig. 2(b), the substrate capacitance C_S for the active region consists of $C_{\rm FREE}$ for free electrons in the conduction band, $C_{\rm LOC}$ for the DOS-induced localized charges (including both interface and bulk traps), and $C_{\rm LOC,ph}$ for the photo-excited electrons from the photo-responsive energy range over the bandgap. The ideality factor $\eta(V_{\rm GS})$, as an indicator for the controllability of the surface potential (ψ_S) by the gate voltage, is dependent on $C_{\rm FREE}$ and $C_{\rm LOC}$.

The subthreshold drain current ($I_{D,{\rm sub}}$) of n-channel a-IGZO TFTs under the gate bias below the threshold voltage($V_{\rm GS} < V_T$) is described by

$$I_{D,{\rm sub}} = \mu_{\rm eff} C_{\rm ox} \left(\frac{W}{L}\right) (\eta(V_{\rm GS}) - 1) V_{\rm th}^2 \times \exp\left(\frac{V_{\rm GS} - V_T}{\eta(V_{\rm GS}) V_{\rm th}}\right) \quad (1)$$

with V_T as the threshold voltage, $\eta(V_{\rm GS})$ as the $V_{\rm GS}$-dependent ideality factor related to $g(E)$ through $C_{\rm LOC}(V_{\rm GS})$, and $V_{\rm th}$ as the thermal voltage, $\mu_{\rm eff}$ as the effective mobility, $C_{\rm ox}(= \varepsilon_{\rm ox}/T_{\rm ox})$ as the oxide capacitance per unit area, and W/L as the gate width/length ratio. In the previous differential ideality factor technique (DIFT) in [9], the contribution from free electrons in the conduction band even under subthreshold bias was neglected ($C_{\rm FREE} \ll C_{\rm LOC}$) and the substrate capacitance (C_S) was modeled to be

$$C_S = \frac{d(Q_{\rm LOC} + Q_{\rm Free})}{d\psi_S} = C_{\rm LOC}(V_{\rm GS}) + C_{\rm FREE}(V_{\rm GS}) \cong C_{\rm LOC}(V_{\rm GS}). \quad (2)$$

Under the gate bias close to the threshold voltage, however, we note that there are considerable free electrons in the channel and $C_{\rm FREE}$ for the free electrons cannot be neglected.

Therefore, by the sub-bandgap photons combined with differential ideality factors, we now propose the sub-bandgap optoelectronic technique for extraction of the intrinsic subgap DOS $g(E)$ excluding the contribution from free electrons (especially for $V_{\rm GS}$ close to V_T) in the conduction band. Substrate capacitance ($C_{S,{\rm dark}}(V_{\rm GS})$, $C_{S,{\rm ph}}(V_{\rm GS})$) and ideality factors ($\eta_{\rm dark}(V_{\rm GS})$, and $\eta_{\rm ph}(V_{\rm GS})$) under dark and under sub-bandgap photonic excitation are described by

$$C_{S,{\rm dark}}(V_{\rm GS}) = C_{\rm LOC}(V_{\rm GS}) + C_{\rm FREE}(V_{\rm GS}) \quad (3)$$

$$C_{S,{\rm ph}}(V_{\rm GS}) = C_{\rm LOC}(V_{\rm GS}) + C_{\rm FREE}(V_{\rm GS}) + C_{\rm LOC,ph}(V_{\rm GS}) \quad (4)$$

$$\eta_{\rm dark}(V_{\rm GS}) = 1 + \frac{C_{\rm LOC}(V_{\rm GS}) + C_{\rm FREE}(V_{\rm GS})}{C_{\rm ox}} \quad (5)$$

$$\eta_{\rm ph}(V_{\rm GS}) = 1 + \frac{C_{\rm LOC}(V_{\rm GS}) + C_{\rm FREE}(V_{\rm GS})}{C_{\rm ox}} + \frac{C_{\rm LOC,ph}(V_{\rm GS})}{C_{\rm ox}}. \quad (6)$$

By taking the difference between ideality factors as

$$\Delta\eta(V_{\rm GS}) \equiv \eta_{\rm ph}(V_{\rm GS}) - \eta_{\rm dark}(V_{\rm GS}) = \frac{C_{\rm LOC,ph}(V_{\rm GS})}{C_{\rm ox}} \quad (7)$$

we get $C_{\rm LOC,ph}(V_{\rm GS})$ for the intrinsic $g(E)$ through

$$C_{\rm LOC,ph}(V_{\rm GS}) = C_{\rm ox} \Delta\eta(V_{\rm GS}). \quad (8)$$

We note that the contribution from free carriers, which is common in the dark and in the photonic excitation, is canceled out by taking the difference of ideality factors. This allows a complete de-embedding of the contribution from free electrons in the conduction band even under subthreshold condition. We note that the V_{GS}-dependent ideality factor $\eta(V_{GS})$ can be experimentally obtained from the subthreshold drain current through

$$\eta(V_{GS}) = \left(\frac{(V_{GS}+\Delta V_{GS}) - V_{GS}}{V_{th}}\right) \Big/ \ln\left(\frac{I_{D,sub}(V_{GS}+\Delta V_{GS})}{I_{D,sub}(V_{GS})}\right). \tag{9}$$

For the SODIFT, we employ V_T-independent but V_{GS}-dependent differential change in the difference between ideality factors $(d\Delta\eta(V_{GS})/d(V_{GS}))$ from experimental data. The subgap DOS-induced capacitance $C_{LOC}(V_{GS})$ from (7), governed by V_{GS}-dependent localized charges $Q_{LOC}(V_{GS})$, is described by

$$\frac{d\Delta\eta(V_{GS})}{dV_{GS}} = \frac{1}{C_{ox}}\left(\frac{dC_{LOC,ph}(V_{GS})}{d\psi_S}\cdot\frac{d\psi_S}{dV_{GS}}\right) \tag{10}$$

$$C_{LOC,ph}(V_{GS}) = C_{ox}\int_{\psi_S(V_{GS}=V_{FB})}^{\psi_S(V_{GS})}\left(\frac{d\Delta\eta(V_{GS})}{dV_{GS}}\Big/\frac{d\psi_S}{dV_{GS}}\right)d\psi_S. \tag{11}$$

For a nonlinear mapping of the gate voltage (V_G) to the energy level over the bandgap ($E_V < E < E_C$), the surface potential ψ_S is converted from the experimental I–V characteristics in [10].

Finally, intrinsic DOS $g(E)$ de-embedded the free carrier in the photo-responsive range over the bandgap can be extracted from the experimental data in the subthreshold region though

$$g(E) = \frac{\Delta C_{LOC,ph}(V_{GS})}{q^2 T_{IGZO}}\ [\mathrm{eV}^{-1}\ \mathrm{cm}^{-3}] \tag{12}$$

$$\Delta C_{LOC,ph}(V_{GS}) = C_{ox}\int_{\psi_S(V_{GS})}^{\psi_S(V_{GS}+\Delta V_{GS})}\left(\frac{d\Delta\eta(V_{GS})}{dV_{GS}}\Big/\frac{d\psi_S}{dV_{GS}}\right)d\psi_S \tag{13}$$

with T_{IGZO} as the effective thickness of the active layer. The proposed SODIFT is independent of V_T, and it is useful to extract the energy distribution of $g(E)$ over the bandgap by using the V_{GS}-dependent subthreshold characteristics under sub-bandgap optical illumination.

III. Experimental Results and Discussion

In order to confirm the proposed SODIFT by using sub-bandgap optical source (red) for extraction of intrinsic DOS $g(E)$ over the bandgap after de-embedding the contribution from free electrons as shown in Fig. 2(b), we applied the SODIFT to n-channel a-IGZO TFTs with $W/L/L_{ov} = 30/6/5\ \mu$m and extracted the energy distribution of $g(E)$ for the localized states over the bandgap. The gate dielectric material is SiO_2 with $T_{ox} = 100$ nm.

Fig. 3 shows the drain current increased due to photo-exited carriers from subgap DOS over the photo responsive energy. In Fig. 3(a), the threshold voltage and the subthreshold slope for the a-IGZO TFT were obtained to be $V_T = 0.2$ V and SS = 230 mV/decade, respectively. The inset of Fig. 3 shows a surface potential (ψ_S) to obtain

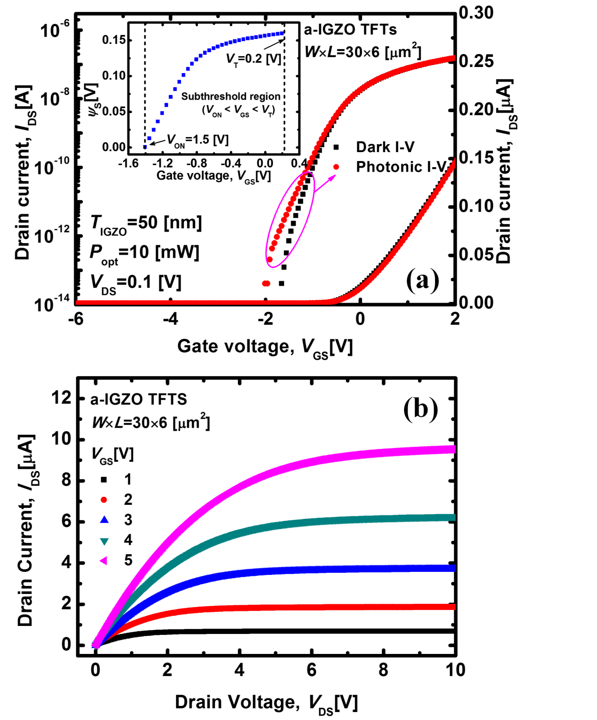

Fig. 3. (a) I_{DS}–V_{GS} curves under dark and photonic states. The $g(E)$ was extracted at maximum optical power to fully pump up electrons from the subgap DOS. The inset shows the surface potential (ψ_S) ($V_{ON} < V_{GS} < V_T$) mapped from I–V curve. (b) I_{DS}–V_{DS} curves under dark state.

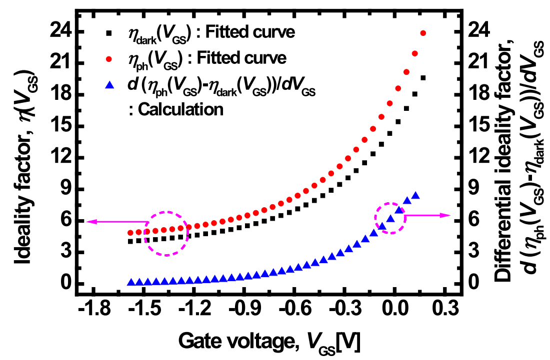

Fig. 4. V_{GS}-dependent ideality factors ($\eta_{dark}(V_{GS})$, $\eta_{ph}(V_{GS})$) and differential ideality factor ($d(\eta_{ph}(V_{GS}) - \eta_{dark}(V_{GS}))/dV_{GS}$) under dark and photonic states.

the energy distribution of $g(E)$ over the bandgap from I–V transfer curve under dark state. Fig. 3(b) shows the output (I_{DS}–V_{DS}) characteristics. In the extraction of the distribution of the intrinsic DOS $g(E)$, SODIFT employs the differentiation of the difference ($\Delta\eta(V_{GS}) = \eta_{ph}(V_{GS}) - \eta_{dark}(V_{GS})$) of ideality factors between dark and sub-bandgap photo-illuminated conditions over the subthreshold bias range ($V_{GS} < V_T$) as shown in Fig. 4.

V_{GS}-dependent experimental ideality factors ($\eta_{dark}(V_{GS})$ under dark and $\eta_{ph}(V_{GS})$ under sub-bandgap photo-illumination are shown in Fig. 4. Extracted $g(E)$ over the bandgap through the proposed SODIFT is shown in Fig. 5 and compared with other extraction method including C_{free} from free electron charges (Q_{free}) for a-IGZO TFTs. The $g(E)$ extraction was performed at maximum optical power to fully pump up carriers in the photo-responsive subgap states.

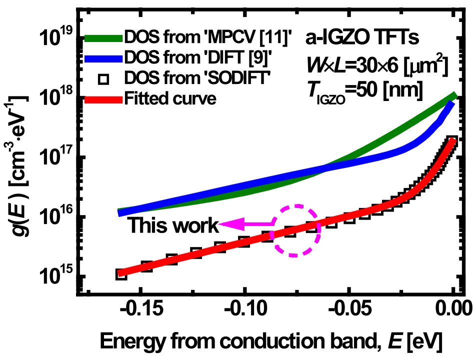

Fig. 5. Intrinsic subgap DOS ($g(E)$) extracted from SODIFT (red line and open symbol) and other method [MPCV (green line) and DIFT (blue line)] for a-IGZO TFTs.

TABLE I
COMPARISON OF EXTRACTED DOS PARAMETERS

DOS / Method	N_{TA}	kT_{TA}	N_{DA}	kT_{DA}
SODIFT	1.7×10^{17}	0.006	2.8×10^{16}	0.05
DIFT [9]	9.2×10^{17}	0.006	1.7×10^{17}	0.05
MPCV [11]	1.0×10^{18}	0.018	6.0×10^{16}	0.10

(Unit : N [eV^{-1}cm^{-3}], kT [eV])

The extracted intrinsic DOS $g(E)$ (red line) close to E_C is empirically modeled to be a superposition of deep and tail states in exponential forms as

$$g(E) = N_{DA} \times \exp\left(\frac{E - E_C}{kT_{DA}}\right) + N_{TA} \times \exp\left(\frac{E - E_C}{kT_{TA}}\right) \quad (14)$$

with $N_{TA} = 17 \times 10^{17}$ cm^{-3} · eV^{-1}, $kT_{TA} = 0.006$ eV, $N_{DA} = 2.8 \times 1^{16}$ cm^{-3} · eV^{-1}, and $kT_{DA} = 0.05$ eV. In Table I, $g(E)$ from the SODIFT is compared with those from the C–V (MPCV [11]) and I–V (DIFT [9]) extraction methods.

We first note that the difference in the extracted $g(E)$ between the SODIFT and the DIFT is mainly caused by the free carriers in the conduction band as expected. The difference is more significant in the subgap states close to E_C, which is mapped from the gate voltage to the surface potential. In addition, a considerable difference at tail states close to E_C between the SODIFT and the MPCV techniques is expected to be induced by multiple causes; one from the free electrons and the other from a configurative factor between I–V and C–V characterization process. In the C–V-based extraction procedure, we expect that there is an inherent component to be corrected for the intrinsic DOS in the active region excluding the contribution from the gate-to-source and gate-to-drain overlapped region [12], [13].

IV. CONCLUSION

We proposed a fully subthreshold current-based SODIFT and the intrinsic subgap DOS by de-embedding the contribution from free carriers in a-IGZO TFTs. The proposed SODIFT is confirmed by application to a-IGZO TFTs for the intrinsic DOS over the bandgap. We expect that the SODIFT is advantageous in the accuracy over the previous C–V-based techniques for AOS TFTs with a small size suppressing any contribution from the overlapped regions as well as the active channel region itself.

REFERENCES

[1] H.-H. Hsieh, T. Kamiya, K. Nomura, H. Hosono, and C.-C. Wu, "Modeling of amorphous InGaZnO$_4$ thin film transistors and their subgap density of states," *Appl. Phys. Lett.*, vol. 92, no. 13, pp. 133503-1–133503-3, Apr. 2008.

[2] A. Suresh and J. F. Muth, "Bias stress stability of indium gallium zinc oxide channel based transparent thin film transistors," *Appl. Phys. Lett.*, vol. 92, no. 3, pp. 033502-1–033502-3, Jan. 2008.

[3] B. Ryu, H.-K. Noh, E.-A. Choi, and K. J. Chang, "O-vacancy as the origin of negative bias illumination stress instability in amorphous In-Ga-Zn-O thin film transistors," *Appl. Phys. Lett.*, vol. 97, no. 2, pp. 022108-1–022108-3, Jul. 2010.

[4] M. Kimura, T. Nakanishi, K. Nomura, T. Kamiya, and H. Hosono, "Trap densities in amorphous-InGaZnO_4 thin-film transistors," *Appl. Phys. Lett.*, vol. 92, no. 13, p. 133512, Apr. 2008.

[5] C. E. Kim *et al.*, "Density-of-states modeling of solution-processed InGaZnO thin-film transistors," *IEEE Electron Devices Lett.*, vol. 31, no. 10, pp. 1131–1133, Oct. 2010.

[6] S. Lee *et al.*, "Extraction of subgap density of states in amorphous InGaZnO thin-film transistors by using multifrequency capacitance–voltage characteristics," *IEEE Electron Devices Lett.*, vol. 31, no. 3, pp. 231–233, Mar. 2010.

[7] H. Bae *et al.*, "Modified conductance method for extraction of subgap density of states in a-IGZO thin-film transistors," *IEEE Electron Devices Lett*, vol. 33, no. 8, pp. 1138–1140, Aug. 2012.

[8] T.-C. Chen *et al.*, "Behaviors of InGaZnO thin film transistor under illuminated positive gate-bias stress," *Appl. Phys. Lett.*, vol. 97, no. 11, pp. 112104-1–112104-3, Sep. 2010.

[9] M. Bae *et al.*, "Differential ideality factor technique for extraction of subgap density of states in amorphous InGaZnO thin-film transistors," *IEEE Electron Devices Lett.*, vol. 33, no. 3, pp. 399–401, Mar. 2012.

[10] S. Jun, C. Jo, H. Bae, H. Choi, D. H. Kim, and D. M. Kim, "Unified subthreshold coupling factor technique for surface potential and subgap density-of-states in amorphous thin film transistors," *IEEE Electron Device Lett.*, vol. 34, no. 5, pp. 641–643, May 2013.

[11] H. Bae *et al.*, "Single-scan monochromatic photonic capacitance–voltage technique for extraction of subgap DOS over the bandgap in amorphous semiconductor TFTs," *IEEE Electron Devices Lett.*, vol. 34, no. 12, pp. 1524–1526, Dec. 2013.

[12] H. Bae *et al.*, "Extraction technique for intrinsic subgap DOS in a-IGZO TFTs by de-embedding the parasitic capacitance through the photonic *C–V* measurement," *IEEE Electron Devices Lett.*, vol. 34, no. 1, pp. 57–59, Jan. 2013.

[13] O. Marinov, M. J. Deen, J. A. J. Tejada, and B. Iniquez, "Impact of the fringing capacitance at the back of thin-film transistors," *Organic Electron.*, vol. 12, no. 6, pp. 936–949, Jun. 2011.

Authors' photographs and biographies not available at the time of publication.